PCCP

ROYAL SOCIETY OF CHEMISTRY

PAPER

View Article Online
View Journal | View Issue

Cite this: *Phys. Chem. Chem. Phys.*, 2020, **22**, 12688

Surface-orientation- and ligand-dependent quenching of the spin magnetic moment of Co porphyrins adsorbed on Cu substrates†

Lucas M. Arruda,[ab] Md. Ehesan Ali,[c] Matthias Bernien,[a] Nino Hatter,[a] Fabian Nickel,[a] Lalminthang Kipgen,[a] Christian F. Hermanns,[a] Timo Bißwanger,[a] Philip Loche,[a] Benjamin W. Heinrich,[a] Katharina J. Franke,[a] Peter M. Oppeneer[d] and Wolfgang Kuch*[a]

Porphyrin molecules are particularly interesting candidates for spintronic applications due to their bonding flexibility, which allows to modify their properties substantially by the addition or transformation of ligands. Here, we investigate the electronic and magnetic properties of cobalt octaethylporphyrin (CoOEP), deposited on copper substrates with two distinct crystallographic surface orientations, Cu(100) and Cu(111), with X-ray absorption spectroscopy (XAS) and X-ray magnetic circular dichroism (XMCD). A significant magnetic moment is present in the Co ions of the molecules deposited on Cu(100), but it is completely quenched on Cu(111). Heating the molecules on both substrates to 500 K induces a ring-closure reaction with cobalt tetrabenzoporphyrin (CoTBP) as reaction product. In these molecules, the magnetic moment is quenched on both surfaces. Our XMCD and XAS measurements suggest that the filling of the d_{z^2} orbital leads to a non-integer valence state and causes the quench of the spin moments on all samples except CoOEP/Cu(100), where the molecular conformation induces variations to the ligand field that lift the quench. We further employ density functional theory calculations, supplemented with on-site Coulomb correlations (DFT+*U*), to study the adsorption of these spin-bearing molecules on the Cu substrates. Our calculations show that charge transfer from the Cu substrates as well as charge redistribution within the Co 3d orbitals lead to the filling of the Co minority spin d_{z^2} orbital, causing a 'turning off' of the exchange splitting and quenching of the spin moment at the Co magnetic centers. Our investigations suggest that, by this mechanism, molecule–substrate interactions can be used to control the quenching of the magnetic moments of the adsorbed molecules.

Received 14th February 2020,
Accepted 18th May 2020

DOI: 10.1039/d0cp00854k

rsc.li/pccp

I. Introduction

The magnetic properties of single molecules have been avidly studied in recent years due to their prospective applications in magnetic spintronic devices. Their proposed uses include magnetic data storage and processing, with additional applications being discovered as the field matures.[1] In the search for molecules that are well suited for the production of such devices, it is fundamental to understand how their magnetic state is affected by their components, such as organic ligands and magnetic centers as well as the environment, as these characteristics will dictate which molecules are suitable for a given application and under which conditions. The bonding flexibility of metalloporphyrin molecules, for instance, makes them versatile candidates for spintronic applications.[2–5] The magnetic properties of these molecules, which result from the metallic ions at their center, can be readily influenced by changes to the molecules' ligands.[6–9]

While there are molecules with properties that remain largely unchanged by their contact with metallic substrates,[10] the substrate interaction is among the most important factors in the determination of the magnetic properties of a molecule.[11,12] The degree of molecule–substrate interaction varies for different substrates. Molecules deposited on weakly interacting substrates often display properties akin to bulk samples even in submonolayer coverages, but that is not the case for many molecules deposited on metallic substrates.[13,14] Calculations also clearly indicate a stronger interaction with metallic substrates as

[a] *Institut für Experimentalphysik, Freie Universität Berlin, Arnimallee 14, 14195 Berlin, Germany. E-mail: kuch@physik.fu-berlin.de*
[b] *CAPES Foundation, Ministry of Education of Brazil, 70040-020 Brasília-DF, Brazil*
[c] *Institute of Nano Science and Technology, Phase-10, Sector-64, Mohali-160062, Punjab, India*
[d] *Department of Physics and Astronomy, Uppsala University, Box 516, 75120 Uppsala, Sweden*

† Electronic supplementary information (ESI) available. See DOI: 10.1039/d0cp00854k

compared to graphite.[15] Additional control of the magnetic properties of a molecule can consequently be achieved by the introduction of buffer layers, such as oxygen[2] or graphene. The latter has been shown to alter or disrupt some interactions of molecules with metallic substrates.[16,17] In particular, the electronic and magnetic properties of cobalt octaethylporphyrin (CoOEP) were shown to depend crucially on the substrate.[18] Whereas Au(111) substrates hardly perturbed the electronic structure and magnetic properties, Ag(111) and Ag(110) substrates led to hybridization and charge transfer to the molecule.[19]

In a simple picture, the substrate can be regarded as an axial ligand to the porphyrin core. Axial ligand manipulation is a well-known strategy for spin-state manipulation. An alternative method of modifying the electronic and magnetic properties of molecules is to alter their equatorial ligands,[20] which can be achieved post-deposition on a substrate, by subjecting the molecules to chemical reactions.[21–25] These two aspects of molecular manipulation are closely interdependent because the ligand determines also the hybridization strength with the substrate. In this work we set out to investigate how these two types of manipulation can lead to major modifications of the properties of the magnetic center of metallorganic porphyrin molecules. To this end, we deposit CoOEP molecules on Cu(100) and Cu(111) and determine their electronic and magnetic properties by X-ray absorption (XA) techniques. Interestingly, the change of surface orientation from Cu(100) to Cu(111) leads to quenching of the magnetic moment. Imposing a thermally-induced ring-closure reaction on the molecular ligands results in a vanishing magnetic moment of the Co center also on Cu(100). Such a ring closure has been described for an FeOEP molecule on different substrates[26,27] in scanning tunneling microscopy (STM) studies, and it has been shown to promote a significant alteration of the magnetic anisotropy of the central ion post reaction.[28]

We seek, furthermore, to explain the mechanism behind these changes with the aid of density functional theory with on-site Coulomb correlations (DFT+U). The calculations show that the quench of the moment post-reaction can be attributed to hybridization with the substrate, particularly through the d_{z^2} orbital of the ion. Although the interaction with the Cu(100) and Cu(111) is not seen to be exactly the same, in both cases the moment is quenched by the same mechanism.

II. Experimental section

The X-ray absorption spectroscopy (XAS) and X-ray magnetic circular dichroism (XMCD) measurements were performed at BESSY II, the Berlin Electron Storage Ring for Synchrotron Radiation, at the UE46_PGM-1 beamline. The energy resolution was set to 160 meV, providing a flux of 10^{10} ph per s. A relatively large spot size of about 1 mm^2 was used to minimize radiation damage to the molecules. The signal, obtained by total electron yield, was normalized first with the signal from a freshly evaporated Au grid placed upstream from the experiment, then with the spectra of the corresponding clean substrate.

Samples were prepared by sublimating the commercially available CoOEP molecules in powder form, purchased from Sigma-Aldrich, from a Knudsen cell heated to 510 K onto single crystal copper substrates to a coverage of about 0.5 ML. The coverage was monitored with a quartz microbalance and cross-checked with intensity calibration of the cobalt and nitrogen absorption edges. The substrates have been previously cleaned by cycles of argon sputtering (1.5 kV, $p_{Ar} = 8 \times 10^{-5}$ mbar, 300 K) and annealing (940 K) and were kept at room temperature in a pressure range of 1×10^{-9} mbar during deposition. The measurements are performed in a 1×10^{-10} mbar pressure range and at temperatures between 4 K and 6 K, determined by a thermocouple placed near the sample shuttle.

The spectra were taken with an external magnetic field of 6 T along the direction of X-ray incidence, unless stated otherwise, and the circularly polarized radiation had a degree of polarization of 85%. The grazing measurement angles were different depending on the substrate. Cu(100) grazing measurements were taken at a 20° incidence angle from the surface, while Cu(111) ones were taken at 25°.

III. Theoretical modeling

Theoretical modeling has been performed on the basis of density functional theory with on-site Coulomb correlations (DFT+U). Specifically, we have employed the Perdew–Burke–Ernzerhof (PBE)[29] parametrization for the exchange–correlations potentials in the generalized gradient approximation (GGA). The effective Coulomb correlation applied was $U_{eff} = 3.0$ eV for all the reported calculations, a value that has been shown to be appropriate for metalloporphyrins and phthalocyanines (see ref. 30–32). In these investigations, an empirical way of determining the Hubbard U was used, by comparison of calculated data with known magnetic and structural data. We note that there are also other, non-empirical methods to determine the Hubbard U value.[33,34] All calculations were performed with the Vienna ab initio simulation package (VASP).[35,36] A kinetic energy cutoff of 450 eV was applied for the used projector augmented-wave (PAW) pseudopotentials.[37] To model the molecule–substrate interactions in a systematic manner, Grimme's pair-wise dispersion interactions included in the D2 method[38] were applied in all calculations. The substrate surfaces are constructed by three slab layers consisting of 192 Cu atoms. Full structural optimization of the complete molecule, the position of the molecule with respect to the substrate, and the hybrid interfaces was performed while keeping the bottom layer of Cu atoms fixed. Starting from an adsorption site in which the Co atom laterally sits in between the hollow sites of the first and second substrate layer, the whole system was relaxed by an optimization routine exploring global minima of the system's total energy.

IV. Results and discussion

Room-temperature deposition of CoOEP molecules on Cu(100) and Cu(111) substrates results in flat-lying adsorption configurations (see ESI† for STM images). Fig. 1 shows the X-ray

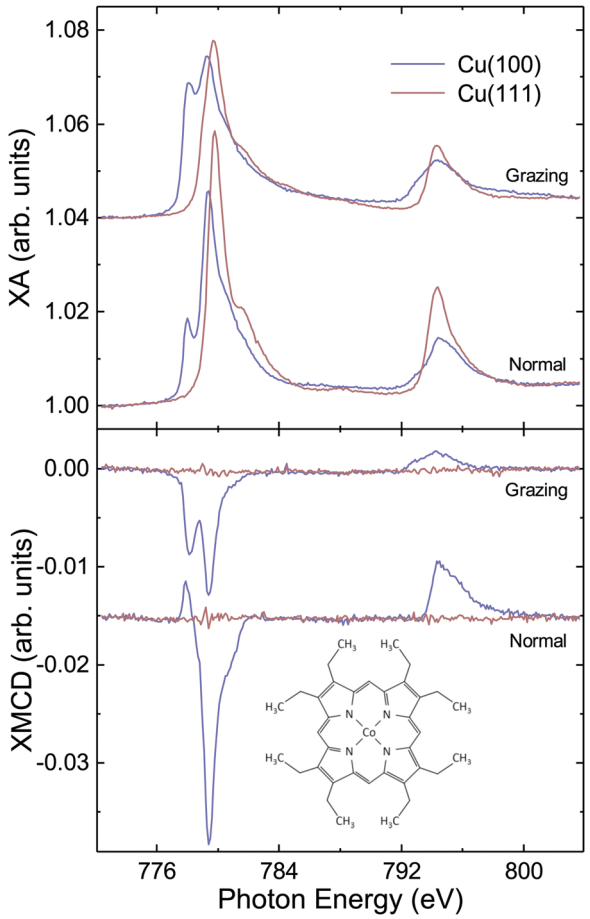

Fig. 1 XA (top) and XMCD (bottom) spectra of CoOEP molecules deposited on Cu(100) and Cu(111) for grazing and normal incidence angles of the X-rays from the substrate. T = 4.4 K and B = 6 T for all spectra. The structure of CoOEP is shown in the inset. Spectra for grazing (top) and normal (bottom) incidence are shifted vertically for clarity.

absorption spectra obtained on both substrates (top) and the corresponding X-ray magnetic circular dichroism (XMCD, bottom) for grazing and normal incidence angles of X-rays. The Co $L_{2,3}$ XA spectra in Fig. 1 (top) display significant differences between the molecules deposited on different substrates. On Cu(100) the spectra have two clearly distinct peaks, at 778.0 eV and 779.4 eV, while on Cu(111) they have one, more intense, peak at 779.8 eV with a pronounced shoulder at 781.6 eV. The peak at 778.0 eV, only present in the spectra of the molecules adsorbed on Cu(100), exhibits a strong angle dependence, suggesting a considerable out-of-plane component. We may hence associate it to the d_{z^2} orbital. Its absence on the Cu(111) surface indicates that this orbital is completely filled in this case.

XMCD spectra displayed in the bottom part of Fig. 1 show a significant dichroic signal for grazing and normal incidence angles on Cu(100), reflecting a sizable magnetic moment of Co. In contrast, the XMCD signal is absent in the same molecules on Cu(111), indicative of a completely quenched magnetic moment. Most probably, the drastic difference in d-orbital structure seen in the XA spectra can be directly related to the different magnetic moments. The XMCD signal on Cu(100) obtained under normal incidence is stronger than the one from grazing incidence, reflecting the dominant contribution of the in-plane orbitals to the total magnetic moment of the molecule. The (smaller) contribution of the out-of-plane orbitals is evidenced by the negative XMCD signal at the L_3 edge at 778.0 eV, a behavior characteristic to the d_{z^2} orbital under normal incidence. The absence of this contribution when the molecules are deposited on Cu(111) is again a strong indication of the complete filling of the d_{z^2} orbital on this substrate. This could, in principle, be caused by a modification of the ligand-field splitting acting on the energy levels of the Co ion when the molecules are deposited on Cu(111). For instance, an enhancement of the equatorial ligand field, stemming from alterations in the conformation of the ethyl groups of the porphyrin macrocycle, could raise the energy of the in-plane orbitals in such a way that the d_{z^2} orbitals becomes fully occupied. Alternatively, a reduction of the axial ligand field caused by a distinct interaction with the substrate would lead to a similar result.

For an integer oxidation state, however, the filling of the d_{z^2} orbital by d-orbital reorganization alone cannot explain the quench of the magnetic moment of the molecule deposited on Cu(111). If the oxidation state of the Co ion were 2+, the same as in the free molecule,[19] any simple charge reorganization would leave the ion with a minimum spin moment S = 1/2 due to the odd number of electrons in the 3d shell. A change in the occupation of the d orbitals stemming from charge transfer with the substrate or the molecular macrocycle is necessary to allow for the quench. To check for a difference in the charge of the Co ion s of the molecules deposited on the two substrates, we analyze the relative d orbital populations. The 3d orbitals' total occupation is obtained from the integrated intensity of the linear-polarization XA spectra under the magic angle of incidence, 54.7° from the surface (see ESI† for spectra), which are equivalent to the isotropic spectra. There is an increase of 9(±3)% in the total integrated intensity of the Co $L_{2,3}$ edge spectra on the Cu(111) substrate compared to the Cu(100) substrate. For grazing incidence, the horizontal-polarization spectra, which probe primarily the out-of-plane orbitals, show a 9(±3)% decrease in intensity when going from Cu(100) to Cu(111), while the vertical-polarization spectra, which probe mainly in-plane orbitals, register a 26(±3)% increase in intensity at grazing incidence, albeit with the 5° difference between the grazing measurements in the different substrates mentioned in section II. This suggests a charge reorganization within the orbitals of the Co ion, with electron transfer from in-plane to out-of-plane orbitals, in addition to a difference of a small fraction of an electron in its total charge. Hence, the oxidation state of the metal center of CoOEP is approximately the same on the two substrates. As mentioned before, the complete quench of the spin magnetic moment observed for the molecules deposited on Cu(111) requires a change in the oxidation state of the Co ion with relation to that of the free molecule, which means that while there is no evidence of a significant difference between the oxidation states of CoOEP

Table 1 Moments obtained from the sum-rule analysis for CoOEP on Cu(100) at 4.4 K and 6 T

α	$\langle m_L(\alpha)\rangle/n_h\mu_B$	$\langle m_S^{eff}(\alpha)\rangle/n_h\mu_B$
90°	0.05 ± 0.01	0.53 ± 0.02
35.3°	0.10 ± 0.01	0.41 ± 0.01
20°	0.11 ± 0.01	0.34 ± 0.03

deposited on the two substrates, it cannot be the same as that of the free molecule. As will be discussed later, the combination of the results of our DFT+U calculations and a sum-rule analysis of the XMCD spectra points to a non-integer valence state between 1+ and 2+ oxidation states. Only in the case of CoOEP deposited on Cu(100), this quench of the magnetic moment induced by the interaction with the substrate does not occur, likely due to ligand-field alterations discussed previously.

To determine the magnetic moments of the CoOEP molecules on Cu(100), the only system in this study in which they are not quenched, we apply a sum-rule analysis.[39,40] The results are compiled in Table 1. The magnetic orbital and effective spin moment components in the direction of the field are given by $\langle m_L(\alpha)\rangle$ and $\langle m_S^{eff}(\alpha)\rangle$, respectively. To obtain the actual magnetic moments, the values in Table 1 must be multiplied by the number of holes n_h in the valence shell of the Co ion (see ESI†). The number of holes in the d orbitals depends on the oxidation state. We will discuss possible oxidation states and how these would affect the interpretation of the magnetic moment in the following. Before doing so, we note that $\langle m_S^{eff}(\alpha)\rangle = \langle m_S(\alpha)\rangle$ only for the measurements taken at the magic angle, where the magnetic dipole operator contribution (T_z) cancels out.

If we assume three holes in the d shell, which would correspond to the oxidation states of 2+, like in the free molecule, we obtain a lower limit for $\langle m\rangle$ of $\langle m\rangle = 1.5(1)\ \mu_B$. Neglecting anisotropy as a first approximation, the Brillouin function for the magnetic moment component in the direction of the field at the temperature and magnetic field conditions of the measurement (see ESI†) yields an unsaturated magnetization that would only agree with this result for an intermediate spin value of $S = 0.85$. This is again a strong indication that the oxidation state of the Co ion is not the same as in the free molecule, where the spin is $S = 1/2$ (see ESI†).

Next, we consider reduction of the Co ion as it has been observed for CoOEP molecules on Ag.[19,41] A full reduction to an oxidation state 1+ is not immediately compatible with the results from the sum-rule analysis, because then the two holes in the d shell would give an unsaturated spin moment $\langle m_S\rangle = 0.82(2)\ \mu_B$. Assuming an 82% saturation of the magnetic signal at 4.4 K and 6 T, this would be consistent with a spin $S = 1/2$, which however is not trivially accessible in this oxidation state due to the number of 3d electrons. For a spin moment of $S = 1$ the assumption of an unrealistically low saturation of only 41% would be required. If we eventually consider the oxidation of the Co ion to be 3+, the results from the sum-rule analysis would be in good agreement with a spin state of $S = 1$. This oxidation state has not been observed for CoOEP molecules deposited on other substrates,[42,43] but it is important to note that it has been observed for CoOEP molecules due to ligand adsorption.[44] As will be later discussed on the basis of the DFT+U results, a fractional charge transfer between central ion and substrate, resulting in a non-integer valence state, with an oxidation state between 1+ and 2+, is favoured by theory. This non-integer valence state allows for the quench of the spin on Cu(111), while on Cu(100), there is a magnetic moment, with a spin value between $S = 1/2$ and $S = 1$. Alternatively, also a mixed-valence state, as discussed by Stepanow *et al.* for CoPc/Au(111),[45] could be possible, in which an electron is delocalized between the substrate and the Co ion. This could also lead to a quenching of the Co magnetic moment.[45]

To understand better the paramagnetic properties of the metal ion on the Cu(100) surface, the integrated intensity of the Co L_3 edge XMCD is taken at different magnetic field values up to the maximum available field of 6 T. The spin Hamiltonian formalism is then used to fit the experimental values of the magnetization obtained from the XMCD:

$$\mathcal{H} = \mu_B g \boldsymbol{B}\cdot\boldsymbol{S} + D S_z^2, \quad (1)$$

where the first term represents the Zeeman energy (μ_B is the Bohr magneton, $\boldsymbol{B}$ is the external field vector and $\boldsymbol{S}$ the spin vector), while the second one describes the uniaxial anisotropy energy (D is the zero-field-splitting parameter and S_z the spin component perpendicular to the plane of the molecule). We assume $g = 2$ for simplicity. As discussed before, the system is likely in an intermediate spin state between $S = 1/2$ and $S = 1$. While a fit according to eqn (1) is not possible for an intermediate value, a reasonable fit is obtained for both spin value limits, with the smallest deviation from experiment obtained for $S = 1$. Fig. 2 shows the experimental values as dots for normal incidence and incidence under the magic angle for circular polarization along with the fits resulting when assuming $S = 1/2$ (broken lines) and $S = 1$ (continuous lines). The higher intensity of the saturated value of the integrated XMCD signal under normal incidence relative to the one at magic angle of incidence indicates, as already discussed before with respect to the XMCD spectra in Fig. 1, that the in-plane orbitals are

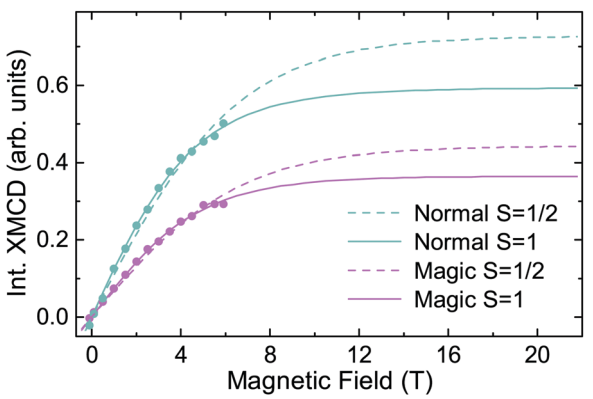

Fig. 2 Magnetization curves for CoOEP on Cu(100) under normal and magic angles of X-ray incidence. The dots are the experimental data, the solid lines are the fitted curves for $S = 1$ ($D = -0.05(10)$ meV), and the dashed lines are the fitted curves for $S = 1/2$. $T = 4.4$ K.

predominantly responsible for the magnetic signal. The relative saturation and curvature, on the other hand, are similar for both incidence angles, which indicates small magnetic anisotropy. This is confirmed by the very low value $D = -0.05 \pm 0.1$ meV obtained for the magnetic anisotropy for $S = 1$ from the fitting procedure. The difference in the XMCD signal between the two angles of incidence is thus also in the case of $S = 1$ accounted for mostly by the magnetic dipole operator, which arises from the XMCD measurement, and represents the spin density anisotropy.[46] As discussed before, the saturation for magic-angle incidence has to be compatible with the result of the sum-rule analysis of the XMCD signal, which depends on the number of unoccupied 3d states. This is only the case for a noninteger 3d occupation between 7 and 8 and a spin state between 1/2 and 1.

In order to get a deeper insight into the influence of the macrocycle ligands on the properties of the central ion, a thermally induced ring-closure reaction from CoOEP to cobalt tetrabenzoporphyrin (CoTBP) was performed. The annealing was done in a stepwise manner. During the last step, in which the sample was kept at a temperature of roughly 500 K for 15 minutes, the changes in the nitrogen K edge spectrum reached saturation. The characteristic changes in the electronic structure of the nitrogen atoms of the molecular macrocycle, as well as additional STM experiments (see ESI†), confirm that the reaction took place. The XA and XMCD spectra after the ring closure are shown in Fig. 3. Similar to the case of the CoOEP molecules on the two copper substrates, there are only small differences in the integrated intensity of the magic-angle incidence spectra between the two substrates (see ESI†). Hence, the difference in charge transfer between the different substrates is again only of the order of a small fraction of an electron. On Cu(100), the integrated intensity is increased by 12(±3)% for CoTBP as compared to CoOEP, while on Cu(111), there is a 9(±3)% reduction. While there is no significant change in line shape between the spectra of CoOEP and CoTBP on Cu(111), the CoTBP spectra on Cu(100) are significantly different from the CoOEP ones on the same substrate. The main discernible feature when comparing the spectra of the CoTBP molecules on the two substrates is that the ones on Cu(100) exhibit a slightly broader and less intense main peak, reminiscent of CoOEP, but now shifted to higher energies and better matching the spectra of CoTBP on Cu(111). This small difference in the electronic structure, however, is not observable in the XMCD spectra, because the CoTBP molecules possess quenched spin magnetic moments on both substrates.

Next, we discuss the results of DFT+U calculations, which are able to explain the spin quenching mechanism of the CoTBP molecules on the two Cu substrates. The spin moment reduction observed for CoOEP on Cu(111), however, is not well described, as outlined below. In Fig. 4 we show the calculated local density of states (DOS) of the free CoTBP molecule, as well as when it is deposited on Cu(100) and Cu(111). The 3d electronic configuration of the free CoTBP molecule is calculated to be $(d_{xy})^2$, $(d_{xz})^2$, $(d_{yz})^2$, $(d_{z^2})^1$, $(d_{x^2-y^2})^0$. This corresponds to a spin moment $S = 1/2$ for the free molecule, due to the half-filled d_{z^2} orbital. When the molecule is deposited on either substrate, the d_{z^2} orbital hybridizes and becomes filled with charge contributions from other d orbitals and from the copper surface, which occurs mainly through the out-of-plane orbitals. The electron charge transfer from the substrates to the molecules, calculated using Bader's analysis, is given in the ESI.† We find a net transfer of 0.43 and 0.34 electrons from the substrate to the molecule for CoTBP/Cu(001) and CoTBP/Cu(111), respectively, while the number of electrons in the Co 3d orbitals decreases by 0.09 electron on Cu(100) and increases by 0.29 electron on Cu(111) (see ESI†). The full occupation of the d_{z^2} orbital is reflected in the experiment by the lack of the characteristic peak at around 778 eV in Fig. 3, and is the primary cause for the quench of the spin moment on both substrates. The charged nature of the molecules is also seen in STM images of both molecules on the two substrates, shown in the ESI,† as the separation between the molecules observed is characteristic of intermolecular electrostatic repulsion.

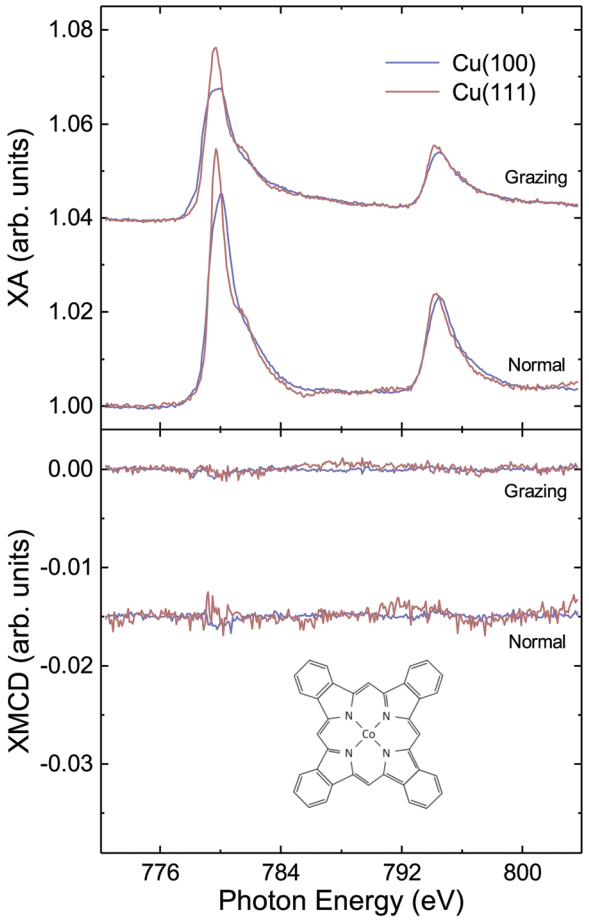

Fig. 3 XA (top) and XMCD (bottom) spectra of CoTBP molecules measured on Cu(100) and Cu(111) for grazing and normal incidence angles of the X-rays to the substrate. $T = 5.8$ K and $B = 6$ T for all spectra. The structure of CoTBP is shown in the inset. Spectra for grazing (top) and normal (bottom) incidence are shifted vertically for clarity.

The calculated spin density plots, shown in Fig. 5, indicate a much more dispersed spin density on the Cu(100) substrate than on Cu(111). This, however, does not affect the overall

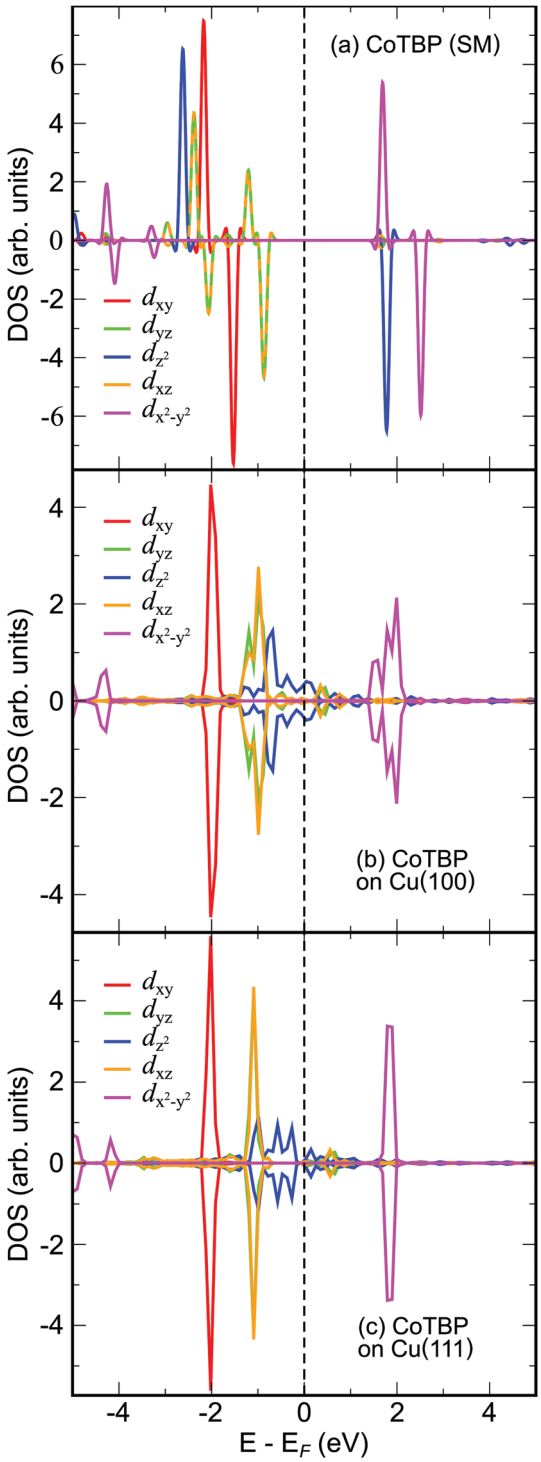

Fig. 4 Calculated local 3d-DOS of the Co atom in gas-phase CoTBP molecule (a), CoTBP deposited on Cu(100) (b), and CoTBP deposited on Cu(111) (c). Note the change in the d_{z^2} orbital when the CoTBP molecule is adsorbed on the Cu substrates. Top panels show majority spin 3d DOS, bottom panels minority spin DOS.

quenching of the spin moment on the two substrates. The spin-density values are extremely small, likely caused by a breaking in symmetry due to molecule–substrate interactions. The presence of a non-zero spin density confirms the open-shell

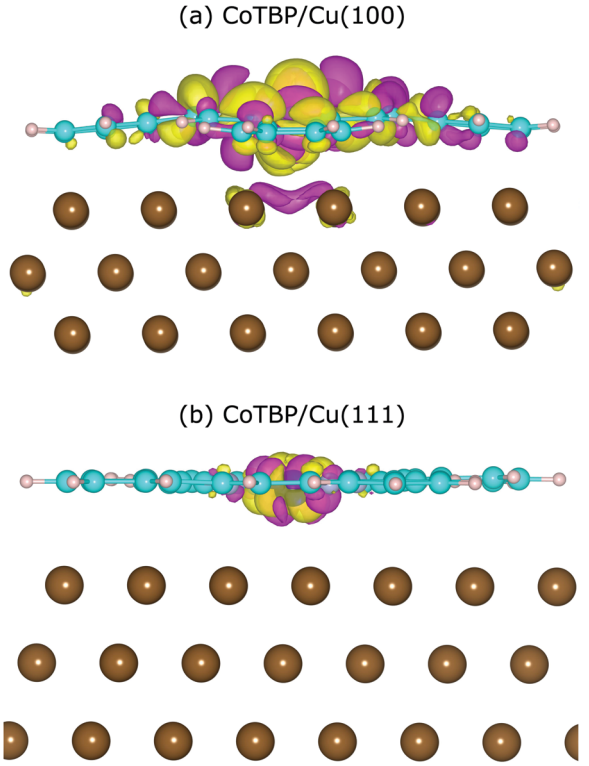

Fig. 5 Spin density plots of the CoTBP molecule deposited on Cu(100) (a) and on Cu(111) (b). The contour value is 1×10^{-7} μ_B Å^{-3}.

nature of the molecule even though the magnetic moments are quenched. As a further difference, CoTBP on Cu(100) undergoes a stronger buckling than CoTBP on Cu(111), evidenced by the larger difference between the distance to the first copper layer of carbon atoms in the macrocycle ring and the ones in the benzene ring, see Fig. 5. On the Cu(100) substrate this difference is around 0.3 Å, while on Cu(111), it is only about 0.05 Å. This leads to a modified hybridization of the d_{xz} and d_{yz} orbitals, making these orbitals distinct, as can be seen from the local DOS in Fig. 4. Also the different lateral position of the Co atom relative to the Cu atoms on the two substrates (see ESI†) could influence the charge transfer to the Co $3d_{z^2}$ orbital.[47] The concurrent spin transfer from substrate to the molecule causes the substrate atoms (especially on the 2nd layer from the surface) to become slightly spin-polarized. This spin polarization is distributed over a range of Cu atoms underneath the molecule.

The situation is different for CoOEP on Cu(100) and Cu(111). Our DFT+U calculations predict a spin moment quench for the CoOEP when deposited on Cu(100), and a strong reduction when deposited on Cu(111). This behavior is not the one observed in the XMCD measurements described above, where the quench of the molecular spin moment is observed on Cu(111), but not on Cu(100). Local DOS plots of the CoOEP molecule in gas phase and on the two substrates are presented in the ESI,† along with calculated spin density plots for the two substrates. The calculated mechanism of the quench is the same as for CoTBP, namely the filling of the Co $3d_{z^2}$ orbital. As mentioned above, a filling of the d_{z^2} orbital accompanying

the quench of the Co magnetic moment in CoOEP is also observed experimentally, albeit not on the same system as predicted by our calculations. Calculating the electron charge transfer from the substrates to the molecule (see ESI†) we find a net transfer of 0.16 and 0.31 electrons for CoOEP/Cu(111) and CoOEP/Cu(001), respectively. The computed smaller charge transfer from the Cu(111) substrate to the molecule is not sufficient to fill the empty d_{z^2} orbital and the molecule retains its spin moment in the calculation.

There could be various reasons for the disagreement between the magnetic moment on the Co atom in CoOEP/Cu(100) and CoOEP/Cu(111) computed by DFT+*U* and the XMCD measurements. The flexible ethyl groups of the CoOEP could play a role in the surface adsorption and this might not be captured consistently by the DFT+*U* calculations. Due to the high complexity of this geometric configuration, the optimized configuration in the calculation could be trapped in such a way that it promotes a slightly unphysical electron transfer to the Co atom of CoOEP/Cu(100) that 'turns off' the exchange splitting [see ESI† Fig. S5(c)]. Another explanation could be that there is a $d^7 + d^8$ mixed-valence behavior of CoOEP on Cu(111), which is not sufficiently described by the static orbital occupations computed with DFT+*U*. Nevertheless, this illustrates that the molecule–substrate interaction is not perfectly described by DFT+*U* for the CoOEP molecule on Cu substrates. In contrast to CoOEP, CoTBP is a very flat molecule that is not expected to have much flexibility in its adsorption geometry. While there are not many calculations in literature for CoTBP, cobalt phthalocyanine (CoPc), a molecule very similar structurally, is usually found to have minimum energy in equivalent configurations on various different substrates,[48–50] with only small deviations to its planarity. The most likely scenario is thus that the non-integer valence state is found on all four systems, but while the adsorption geometry of CoOEP on Cu(111) and CoTBP on both Cu substrates is similar, on Cu(100) the ethyl groups of CoOEP arrange in a less planar structure, leading to less d-orbital repopulation and preventing the quench of the magnetic moment.

Overall, while the theoretical results describe well the experimental observations for CoTBP with respect to orbital filling, in particular the role of the out-of-plane components, the remaining discrepancy on the spin state in CoOEP on the two Cu substrates between theory and experiment further emphasizes the intriguing sensitivity of the Co magnetic moment to tiny changes in the environment, such as the crystallographic orientation of the substrate.

V. Conclusions

From the investigation of the electronic and magnetic properties of the CoOEP/TBP molecules by means of XAS and XMCD, we have demonstrated two ways of completely quenching the spin magnetic moment of a single molecule deposited on metallic substrates.

We have shown that CoOEP deposited on copper displays a non-integer valence configuration that leads to an intermediate spin magnetic moment, caused by the hybridization of the Co ion with the copper substrates. Furthermore, while on Cu(100) a significant magnetic moment is observed, on Cu(111) the Co ions' magnetic moment is fully quenched. CoTBP molecules, obtained through an intramolecular reaction activated by heat, display a quenched moment on both substrates. The similarities between the magnetic and electronic properties of the three systems displaying quenched moments suggest a surprisingly similar ligand field and substrate interaction, indicating that the same mechanism is responsible for the quench of the magnetic moment in the three systems. DFT+*U* calculations show that a hybridization and concurrent fractional charge transfer between molecule and substrate through the out-of-plane orbitals along with a charge reorganization within the Co 3d orbitals is the primary mechanism behind the quench of the magnetic moment in the TBP molecules and, supposedly, also on CoOEP on Cu(111). The XA spectra indicate that the electronic and magnetic differences between CoOEP on the two copper substrates are caused by conformation-induced ligand-field variations rather than by significant changes in the total Co 3d occupation. However, the interaction of the OEP molecules with the two different copper substrates is still not completely understood from our calculations, most likely because of the increased complexity introduced by the ethyl groups of these molecules, whose flexibility may not be fully captured by the DFT+*U* model.

These results add an interesting piece in the puzzle of understanding molecule–substrate interactions and their effect on the properties of magnetic molecules. The differences among all systems studied here are seen to stem mainly from variation of the molecular conformation and intramolecular bonds, while the interactions between the copper surfaces and Co ions, albeit strong and crucial for the realization of the magnetic moments observed, are shown to vary little.

Conflicts of interest

There are no conflicts to declare.

Acknowledgements

The authors would like to gratefully acknowledge the financial support by CAPES (No. 9469/13-3), BMBF through project VEKMAG (BMBF 05K13KEA and 05K16KE3), DFG through SFB 658 and SFB/TRR 227, and the Indo-Swedish Research Collaboration, funded through the Swedish Research Council (VR, 2015-06714) and the Department of Science and Technology (DST, Project No. DST/INT/SWD/VR/P-01/2016 and ECR/2016/000362), India. We thank the HZB for the allocation of synchrotron radiation beamtime, Eugen Weschke and Enrico Schierle for the beamline support, and the Swedish National Infrastructure for Computing (SNIC) for computer time.

Notes and references

1 S. J. van der Molen, R. Naaman, E. Scheer, J. B. Neaton, A. Nitzan, D. Natelson, N. J. Tao, H. van der Zant, M. Mayor,

M. Ruben, M. Reed and M. Calame, *Nat. Nanotechnol.*, 2013, **8**, 385–389.
2 M. Bernien, J. Miguel, C. Weis, M. E. Ali, J. Kurde, B. Krumme, P. M. Panchmatia, B. Sanyal, M. Piantek, P. Srivastava, K. Baberschke, P. M. Oppeneer, O. Eriksson, W. Kuch and H. Wende, *Phys. Rev. Lett.*, 2009, **102**, 047202.
3 W. J. Cho, Y. Cho, S. K. Min, W. Y. Kim and K. S. Kim, *J. Am. Chem. Soc.*, 2011, **133**, 9364–9369.
4 Q. Sun, Y. Dai, Y. Ma, W. Wei, L. Yu and B. Huang, *Sci. Rep.*, 2015, **5**, 12772.
5 C. Wäckerlin, K. Tarafder, J. Girovsky, J. Nowakowski, T. Hählen, A. Shchyrba, D. Siewert, A. Kleibert, F. Nolting, P. M. Oppeneer, T. A. Jung and N. Ballav, *Angew. Chem., Int. Ed.*, 2013, **52**, 4568–4571.
6 W. Hieringer, K. Flechtner, A. Kretschmann, K. Seufert, W. Auwärter, J. V. Barth, A. Görling, H.-P. Steinrück and J. M. Gottfried, *J. Am. Chem. Soc.*, 2011, **133**, 6206–6222.
7 C. Wäckerlin, K. Tarafder, D. Siewert, J. Girovsky, T. Hählen, C. Iacovita, A. Kleibert, F. Nolting, T. A. Jung, P. M. Oppeneer and N. Ballav, *Chem. Sci.*, 2012, **3**, 3154–3160.
8 H. C. Herper, M. Bernien, S. Bhandary, C. F. Hermanns, A. Krüger, J. Miguel, C. Weis, C. Schmitz-Antoniak, B. Krumme, D. Bovenschen, C. Tieg, B. Sanyal, E. Weschke, C. Czekelius, W. Kuch, H. Wende and O. Eriksson, *Phys. Rev. B: Condens. Matter Mater. Phys.*, 2013, **87**, 174425.
9 W. Auwärter, D. Écija, F. Klappenberger and J. V. Barth, *Nat. Chem.*, 2015, **7**, 105–120.
10 E. Kiefl, M. Mannini, K. Bernot, X. Yi, A. Amato, T. Leviant, A. Magnani, T. Prokscha, A. Suter, R. Sessoli and Z. Salman, *ACS Nano*, 2016, **10**, 5663–5669.
11 M. Nakamura, R. Imai, N. Hoshi and O. Sakata, *Surf. Sci.*, 2012, **606**, 1560–1564.
12 J. M. Gottfried, *Surf. Sci. Rep.*, 2015, **70**, 259–379.
13 B. W. Heinrich, C. Iacovita, T. Brumme, D.-J. Choi, L. Limot, M. V. Rastei, W. A. Hofer, J. Kortus and J.-P. Bucher, *J. Phys. Chem. Lett.*, 2010, **1**, 1517–1523.
14 H. Peisert, J. Uihlein, F. Petraki and T. Chassé, *J. Electron Spectrosc. Relat. Phenom.*, 2015, **204**, 49–60.
15 B. Chilukuri, U. Mazur and K. W. Hipps, *Phys. Chem. Chem. Phys.*, 2014, **16**, 14096–14107.
16 C. F. Hermanns, K. Tarafder, M. Bernien, A. Krüger, Y.-M. Chang, P. M. Oppeneer and W. Kuch, *Adv. Mater.*, 2013, **25**, 3473–3477.
17 J. Uihlein, H. Peisert, H. Adler, M. Glaser, M. Polek, R. Ovsyannikov and T. Chassé, *J. Phys. Chem. C*, 2014, **118**, 10106–10112.
18 Y. Bai, M. Sekita, M. Schmid, T. Bischof, H.-P. Steinrück and J. M. Gottfried, *Phys. Chem. Chem. Phys.*, 2010, **12**, 4336–4344.
19 M. Fanetti, A. Calzolari, P. Vilmercati, C. Castellarin-Cudia, P. Borghetti, G. D. Santo, L. Floreano, A. Verdini, A. Cossaro, I. Vobornik, E. Annese, F. Bondino, S. Fabris and A. Goldoni, *J. Phys. Chem. C*, 2011, **115**, 11560–11568.
20 L. Bernasconi, M. J. Louwerse and E. J. Baerends, *Eur. J. Inorg. Chem.*, 2007, **2007**, 3023–3033.
21 M. Lackinger and W. M. Heckl, *J. Phys. D: Appl. Phys.*, 2011, **44**, 464011.
22 A. Wiengarten, J. A. Lloyd, K. Seufert, J. Reichert, W. Auwärter, R. Han, D. A. Duncan, F. Allegretti, S. Fischer, S. C. Oh, Ö. Sağlam, L. Jiang, S. Vijayaraghavan, D. Écija, A. C. Papageorgiou and J. V. Barth, *Chem. – Eur. J.*, 2015, **21**, 12285–12290.
23 C. G. Williams, M. Wang, D. Skomski, C. D. Tempas, L. L. Kesmodel and S. L. Tait, *Surf. Sci.*, 2016, **653**, 130–137.
24 Ö. Sağlam, G. Yetik, J. Reichert, J. V. Barth and A. C. Papageorgiou, *Surf. Sci.*, 2016, **646**, 26–30.
25 B. Cirera, N. Giménez-Agulló, J. Björk, F. Martínez-Peña, A. Martin-Jimenez, J. Rodriguez-Fernandez, A. M. Pizarro, R. Otero, J. M. Gallego, P. Ballester, J. R. Galan-Mascaros and D. Ecija, *Nat. Commun.*, 2016, **7**, 11002.
26 B. W. Heinrich, G. Ahmadi, V. L. Müller, L. Braun, J. I. Pascual and K. J. Franke, *Nano Lett.*, 2013, **13**, 4840–4843.
27 D. van Vörden, M. Lange, M. Schmuck, J. Schaffert, M. C. Cottin, C. A. Bobisch and R. Möller, *J. Chem. Phys.*, 2013, **138**, 211102.
28 L. M. Arruda, M. E. Ali, M. Bernien, F. Nickel, J. Kopprasch, C. Czekelius, P. M. Oppeneer and W. Kuch, *J. Phys. Chem. C*, 2019, **123**, 14547–14555.
29 J. P. Perdew, K. Burke and M. Ernzerhof, *Phys. Rev. Lett.*, 1996, **77**, 3865–3868.
30 P. M. Panchmatia, B. Sanyal and P. M. Oppeneer, *Chem. Phys.*, 2008, **343**, 47–60.
31 M. E. Ali, B. Sanyal and P. M. Oppeneer, *J. Phys. Chem. C*, 2009, **113**, 14381–14383.
32 M. E. Ali, B. Sanyal and P. M. Oppeneer, *J. Phys. Chem. B*, 2012, **116**, 5849–5859.
33 M. Cococcioni and S. de Gironcoli, *Phys. Rev. B: Condens. Matter Mater. Phys.*, 2005, **71**, 035105.
34 P. Guss, M. E. Foster, B. M. Wong, F. Patrick Doty, K. Shah, M. R. Squillante, U. Shirwadkar, R. Hawrami, J. Tower and D. Yuan, *J. Appl. Phys.*, 2014, **115**, 034908.
35 G. Kresse and J. Hafner, *Phys. Rev. B: Condens. Matter Mater. Phys.*, 1993, **47**, 558–561.
36 G. Kresse and D. Joubert, *Phys. Rev. B: Condens. Matter Mater. Phys.*, 1999, **59**, 1758–1775.
37 P. E. Blöchl, *Phys. Rev. B: Condens. Matter Mater. Phys.*, 1994, **50**, 17953–17979.
38 S. Grimme, *J. Comput. Chem.*, 2006, **27**, 1787–1799.
39 B. T. Thole, P. Carra, F. Sette and G. van der Laan, *Phys. Rev. Lett.*, 1992, **68**, 1943–1946.
40 P. Carra, B. T. Thole, M. Altarelli and X. Wang, *Phys. Rev. Lett.*, 1993, **70**, 694–697.
41 Y. Bai, F. Buchner, I. Kellner, M. Schmid, F. Vollnhals, H.-P. Steinrück, H. Marbach and J. M. Gottfried, *New J. Phys.*, 2009, **11**, 125004.
42 C. F. Hermanns, M. Bernien, A. Krüger, W. Walter, Y.-M. Chang, E. Weschke and W. Kuch, *Phys. Rev. B: Condens. Matter Mater. Phys.*, 2013, **88**, 104420.
43 K. Flechtner, A. Kretschmann, H.-P. Steinrück and J. M. Gottfried, *J. Am. Chem. Soc.*, 2007, **129**, 12110–12111.
44 C. F. Hermanns, M. Bernien, A. Krüger, J. Miguel and W. Kuch, *J. Phys.: Condens. Matter*, 2012, **24**, 394008.

45 S. Stepanow, P. S. Miedema, A. Mugarza, G. Ceballos, P. Moras, J. C. Cezar, C. Carbone, F. M. F. de Groot and P. Gambardella, *Phys. Rev. B: Condens. Matter Mater. Phys.*, 2011, **83**, 220401.
46 J. Stöhr and H. König, *Phys. Rev. Lett.*, 1995, **75**, 3748–3751.
47 L. Malavolti, M. Briganti, M. Hänze, G. Serrano, I. Cimatti, G. McMurtrie, E. Otero, P. Ohresser, F. Totti, M. Mannini, R. Sessoli and S. Loth, *Nano Lett.*, 2018, **18**, 7955–7961.
48 Y. Cai, J. Song, S. Bao, P. He, F. Hu and H. Zhang, *Chem. Phys. Lett.*, 2014, **609**, 142–146.
49 H. Sun, Z. Liang, K. Shen, J. Hu, G. Ji, Z. Li, H. Li, Z. Zhu, J. Li, X. Gao, H. Han, Z. Jiang and F. Song, *Surf. Sci.*, 2017, **661**, 34–41.
50 T. Schmitt, P. Ferstl, L. Hammer, M. A. Schneider and J. Redinger, *J. Phys. Chem. C*, 2017, **121**, 2889–2895.